



LAWRENCE  
LIVERMORE  
NATIONAL  
LABORATORY

# Nd<sup>3+</sup> ion diffusion during sintering of Nd:YAG transparent ceramics

J. P. Hollingsworth, J. D. Kuntz, T. F. Soules

October 30, 2008

Journal of Physics D: Applied Physics

## **Disclaimer**

---

This document was prepared as an account of work sponsored by an agency of the United States government. Neither the United States government nor Lawrence Livermore National Security, LLC, nor any of their employees makes any warranty, expressed or implied, or assumes any legal liability or responsibility for the accuracy, completeness, or usefulness of any information, apparatus, product, or process disclosed, or represents that its use would not infringe privately owned rights. Reference herein to any specific commercial product, process, or service by trade name, trademark, manufacturer, or otherwise does not necessarily constitute or imply its endorsement, recommendation, or favoring by the United States government or Lawrence Livermore National Security, LLC. The views and opinions of authors expressed herein do not necessarily state or reflect those of the United States government or Lawrence Livermore National Security, LLC, and shall not be used for advertising or product endorsement purposes.

# Nd<sup>3+</sup> ion diffusion during sintering of Nd:YAG transparent ceramics

Joel P. Hollingsworth, Joshua D. Kuntz and Thomas F. Soules

*Lawrence Livermore National Laboratory, NIF and Photon Sciences, L-470, 7000 East Avenue, Livermore, California, 94550, U.S.A.*

*This work performed under the auspices of the U.S. Department of Energy by Lawrence Livermore National Laboratory under Contract DE-AC52-07NA27344.*

(Received 01 November 2008; ....)

Using an electron microprobe, we measured and characterized the Nd<sup>3+</sup> ion diffusion across a boundary between Nd doped and undoped ceramic yttrium aluminum garnet (YAG) for different temperature ramps and hold times and temperatures. The results show significant Nd ion diffusion on the order of micrometers to tens of micrometers depending on the time and temperature of sintering. The data fit well a model including bulk diffusion, grain boundary diffusion and grain growth. Grain boundary diffusion dominates and grain growth limits grain boundary diffusion by reducing the total cross sectional area of grain boundaries.

Ceramic laser amplifier materials have recently been developed with laser performance<sup>i</sup> that rivals single crystals. Transparent ceramics also offer near net shape and relatively fast and robust fabrication processes compared to growing single crystals. Aperture sizes of 10 cm have been realized enabling average powers of > 25 kW<sup>ii</sup>. In addition, ceramics may be fabricated with dopant concentration gradients so as to possibly include photonic patterns, offset non-uniform pumping patterns, create or smooth beam profiles, or favor a particular transverse mode<sup>iii</sup>. However, any tailoring of the dopant profile must take into account the active ion diffusion that occurs during sintering of the ceramic. Ramirez et al.<sup>iv</sup> recently showed using confocal Raman and fluorescence spectroscopy imaging that there was a higher concentration of Nd<sup>3+</sup> in the grain boundaries of transparent ceramic Nd:YAG prepared by blending high purity Y<sub>2</sub>O<sub>3</sub>, Nd<sub>2</sub>O<sub>3</sub> and Al<sub>2</sub>O<sub>3</sub> powders.

Nd<sup>3+</sup> doped yttrium aluminum garnet Y<sub>3</sub>Al<sub>5</sub>O<sub>12</sub> is by far the most common solid-state laser amplifier material. In this study we measured and characterized the Nd<sup>3+</sup> ion diffusion which occurs during vacuum sintering of Nd:YAG laser ceramics. Powders prepared by flame-spray pyrolysis (FSP) from Nanocerox Inc. were layered in a vacuum cold press. The FSP powders showed spherical morphology and were well dispersed with particle sizes of 30-70 nm from scanning electron microscope (SEM) pictures and BET measurements of 27.3 m<sup>2</sup>/g and 31.2 m<sup>2</sup>/g respectively. Without further processing, the layered pellets were pressed to 67 MPa in a 13 mm vacuum die. The samples were then removed and calcined at

1050C and inserted in a tungsten vacuum furnace. Sintering was carried out by ramping the temperature at 1.25 C per minute and a pressure of less than 0.3 mPa to a hold temperature. Samples were heated to temperatures of 1600, 1650, 1700, 1750 and 1780 and held at these temperatures for 4 minutes, 4 hours and 8 hours. Duplicate samples were made for each temperature and hold time. After sintering, samples were cooled at 5 C per minute. The pellets were sectioned and polished perpendicular to the doped/undoped interface, and analyzed by means of an electron microprobe (JEOL, model JXA-8200). All the pellets appeared transparent and showed little or no porosity in the scanning electron microscope (SEM) images except those fired at 1600 and 1650 C for 4 minutes which were white and clearly showed porosity.

To determine if laser quality samples could be made in this way, homogenous 3 mm thick pellets of FSP 0.6at% Nd:YAG powders were pressed as described above and then sintered for 8 hours at 1780 C and hot-isostatically pressed at 1800 C and 200 MPa and polished. These were mounted at Brewster's angle in the center of a 5.3 cm cavity with a 0.8 reflectivity output coupler and pumped with a Ti:sapphire laser (Spectra-Physics 3900) focused to a 0.2 mm spot. Figure 1 shows the lasing power versus pump power of two ceramic samples and a single 1.1 at % Nd:YAG crystal 4.5 mm in thickness. Although the onset of lasing occurs at a higher pump power and the efficiency is lower than the single crystal in part because of the decreased concentration of Nd and the thinner ceramic samples (transmission is ~ 10 %

versus less than 1 % in the case of the crystal) and greater surface and bulk scattering by the ceramic, these samples still show respectable lasing.

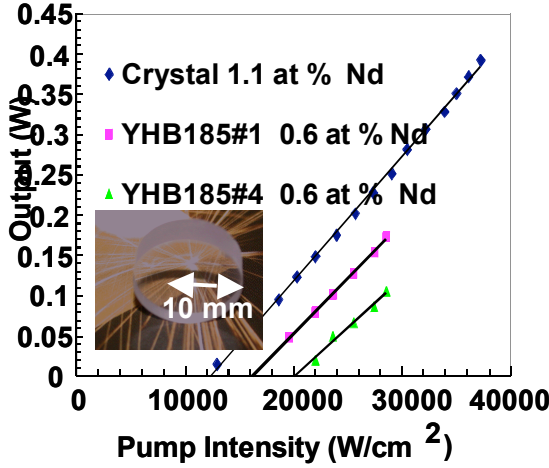


**Figure 1** Laser cavity output versus pump intensity for a single crystal Nd:YAG and ceramic Nd:YAG samples prepared as discussed in the text. Insert is a picture of one of the ceramic samples.

In the presence of a concentration gradient in one dimension, the diffusion equation with a time dependent diffusion coefficient is given by:

$$\begin{aligned} \frac{\partial c}{\partial t} &= D(t) \frac{\partial^2 c}{\partial x^2}; \\ \frac{\partial c}{\partial \tau} &= D_0 \frac{\partial^2 c}{\partial x^2}; \tau = \int f(t) dt \end{aligned} \quad (1)$$

The solution can be written as

$$c = c_0 \left( \frac{1}{2} \right) \left( 1 + \operatorname{erf} \left( \frac{x - \mu}{\sqrt{2D_{eff}t}} \right) \right) \quad (2)$$

where  $\operatorname{erf}$  is the error function,  $c_0$  is the concentration at  $x \ll \mu$ .  $\mu$  is the point where the concentration is  $\frac{1}{2}c_0$ .  $D_{eff}t = \int D(t)dt$ . Eq. 2 provides an excellent fit to the  $\text{Nd}^{3+}$  concentration profile with  $R^2$  (measuring the extent to which the theory accounts for deviations of the data from the mean)  $> 0.997$  for all samples.

Also measurements were made without sintering that show an abrupt demarcation between doped and undoped regions with width equal to the instrument resolution. A representative concentration

profile at 1700 C is shown in Fig. 2 and at different times and temperatures in Appendix A.

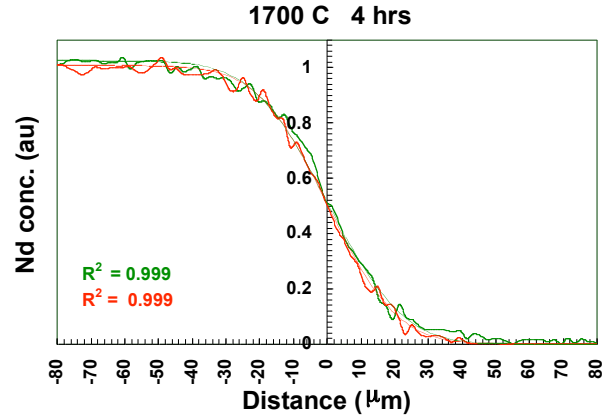


**Figure 2** A graph of  $\text{Nd}^{3+}$  ion concentration profiles measured by the electron microprobe after vacuum sintering. The red and green curves are from two different samples and the  $R^2$  values are computed using Eq. (2) with  $D_{eff}t$  chosen for a best fit.

The diffusion of  $\text{Yb}^{3+}$  into polycrystalline YAG after forming a 10 nm film of  $\text{Yb}_2\text{O}_3$  on the surface was interpreted by M. Jimenez-Melendo and H. Haneda<sup>Error! Bookmark not defined.</sup> in terms of a modification of Fisher's model<sup>v</sup> by A. D. Le Claire<sup>vi</sup>. This leads to a concentration profile versus depth that is nearly exponential with distance. Since our data fits the error function, Eq. 2, very well, we adopted a more heuristic model assuming each atom spends some time diffusing in the bulk (volume diffusion) and in grain boundaries (grain boundary diffusion). Hence the diffusion is represented by the sum of the probability of jumps within the crystallites plus diffusion along grain boundaries. The latter depends on the relative cross sectional area of grain boundaries and varies inversely with the grain size. Hence we can write

$$\begin{aligned} D_{eff}t &= \int_{t(T_0)}^{t_0(T_h)} \left( A e^{\frac{-\Delta E}{R(T_0+rt)}} + \frac{B \delta e^{\frac{-\Delta E'}{R(T_0+rt)}}}{d_0 + \sqrt{ke \frac{-\Delta E''}{R(T_0+rt)}} t} \right) dt \\ &+ \int_{t_0}^{t_f} \left( A e^{\frac{-\Delta E}{RT_h}} + \frac{B \delta e^{\frac{-\Delta E'}{RT_h}}}{d_0 + \sqrt{ke \frac{-\Delta E''}{RT_h}} t} \right) dt. \end{aligned} \quad (3)$$

The first integration is over the ramp from an initial temperature, 1050 C, to the hold temperature ( $r$  is the ramp rate). The second integration is over the hold time.  $\Delta E$ ,  $\Delta E'$  and  $\Delta E''$  are activation energies for volume and grain boundary diffusion and grain growth respectively.  $\Delta E = 567 \pm 15$  kJ/mole was measured on a single YAG crystal with a  $\text{Nd}_3\text{Al}_5\text{O}_{12}$  film using Rutherford backscattering and depth profiling by Cherniak<sup>vii</sup>.  $\delta$  is the grain boundary thickness and the denominators in the grain boundary diffusion terms are proportional to the grain size.  $d_0$  is the initial powder size<sup>viii</sup>.

Eq. (3) can be numerically integrated over both the ramp and hold time for various values of the parameters. Assuming that the initial powder size is small compared to the particle sizes during Nd diffusion, the parameters in Eq. 3 reduce to three. In Fig. 3 the measured values of  $D_{eff}t$  are graphed against calculated values using the best fit three parameters. Data points are for each sample.

$$A = 5.11 \mu\text{m}^2;$$

$$B\delta / \sqrt{k} = 1.01 \times 10^{-5} \mu\text{m}^2 \sqrt{s};$$

$$\Delta E' - \frac{1}{2} \Delta E'' = 249 \text{ kJ}.$$

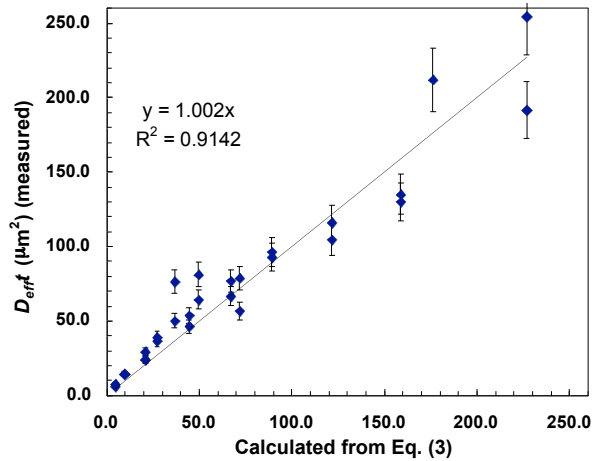


**Figure 3. Measured values of  $D_{eff}t$  versus calculated values for the same ramps and hold times using Eq. 3. All data and results of the calculations are available in Appendix B along with grain sizes .**

Although the model, Eq. 3, is heuristic and does not include surface diffusion (the latter would have the same form as the grain boundary diffusion), the fit is very good over a wide range of experimental

conditions. When graphed on the same chart, bulk diffusion<sup>vii</sup> is one (at low temperatures) to three (at higher temperatures) orders of magnitude less than the grain boundary diffusion so that grain boundary diffusion dominates. The results also show that  $\text{Nd}^{3+}$  diffusion on the order of a couple micrometers occurs even at the lower temperatures, 1600 and 1650 C. At higher temperatures there is significant diffusion with hold times as short as 4 minutes. At long hold times and higher temperatures,  $>1750$  C the diffusion of Nd in these samples is on the order of  $\sqrt{250 \mu\text{m}^2}$ . Hence while composite or graded transparent ceramic parts can be formed in this manner it is unlikely that photonic structures can be fabricated.

<sup>1</sup> A. Ikesue, T. Kinoshita, K. Kamata and K. Yoshida, "Fabrication and Optical Properties of High-Performance Polycrystalline Nd:YAG Ceramics for Solid-State Lasers," J. Am. Ceram. Soc. **78**, 1033-1040 (1993).

<sup>2</sup> T. Soules, "Transparent Ceramics Spark Laser Advances", LLNL Science and Technology Review, 1-6, April 6, 2006.

<sup>3</sup> A. Ikesue and Y. Lin Aung, "Progress in Nd:YAG Ceramic Lasers", 3<sup>rd</sup> Laser Ceramics Symposium, Paris, October 9-10, 2007.

<sup>4</sup> M. O. Ramirez, J. Wisdom, H. Li, Y. Lin Aung, J. Stitt, G. L. Messing, V. Dierolf, Z. Liu, A. Ikesue, R. L. Byer, and V. Gopalan, "Three-dimensional Grain Boundary Spectroscopy in Transparent High Power Laser Materials", OPTICS EXPRESS **16**, 5965-5973 (2008).

<sup>5</sup> J. C. Fisher, "Calculation of Diffusion Penetration Curves for Surface and Grain Boundary Diffusion," J. of App. Phys. **22**, 74-77 (1951).

<sup>6</sup> A. D. Le Claire, "The Analysis of Grain Boundary Diffusion Measurements," Br. J. Appl. Phys. **14**, 351-356 (1963).

<sup>7</sup> D. J. Cherniak, "Rare Earth Element and Gallium Diffusion in Yttrium Aluminum Garnet", Phys. Chem. Materials **26**, 156-163 (1998).

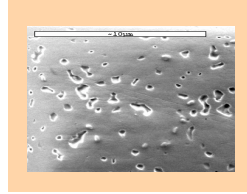
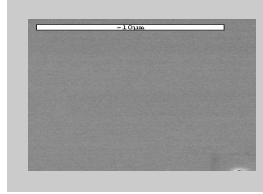
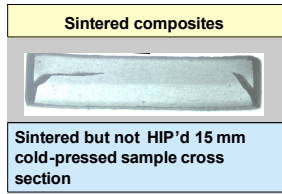
<sup>8</sup> W. D. Kingery, H. K. Bowen and D. R. Uhlman, Introduction to Ceramics, John Wiley and Sons, N.Y. pgs. 448-455 (1976).

## Duplicate set of end notes

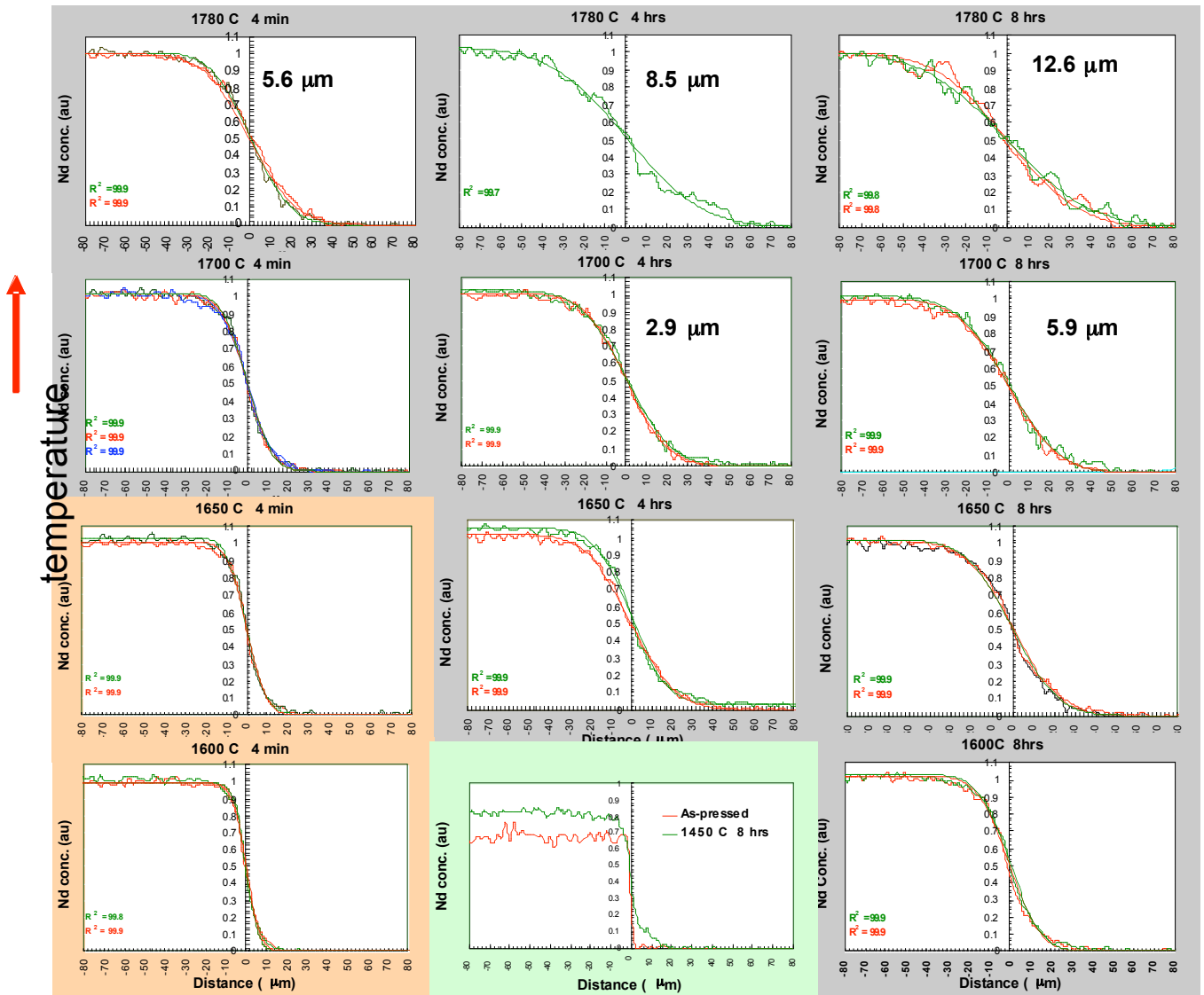
- 
- <sup>i</sup> A. Ikesue, T. Kinoshita, K. Kamata and K Yoshida, "Fabrication and Optical Properties of High-Performance Polycrystalline Nd:YAG Ceramics for Solid-State Lasers," J. Am. Ceram. Soc. **78**, 1033-1040 (1993).
- <sup>ii</sup> T. Soules, "Transparent Ceramics Spark Laser Advances", LLNL Science and Technology Review, 1-6, April 6, 2006.
- <sup>iii</sup> A. Ikesue and Y. Lin Aung, "Progress in Nd:YAG Ceramic Lasers", 3<sup>rd</sup> Laser Ceramics Symposium, Paris, October 9-10, 2007.
- <sup>iv</sup> M. O. Ramirez, J. Wisdom, H. Li, Y. Lin Aung, J. Stitt, G. L. Messing, V. Dierolf, Z. Liu, A. Ikesue, R. L. Byer, and V. Gopalan, "Three-dimensional Grain Boundary Spectroscopy in Transparent High Power Laser Materials", OPTICS EXPRESS **16**, 5965-5973 (2008).
- <sup>v</sup> J. C. Fisher, "Calculation of Diffusion Penetration Curves for Surface and Grain Boundary Diffusion," J. of App. Phys. **22**, 74-77 (1951).
- <sup>vi</sup> A. D. Le Claire, "The Analysis of Grain Boundary Diffusion Measurements," Br. J. Appl. Phys. **14**, 351-356 (1963).
- <sup>vii</sup> D. J. Cherniak, "Rare Earth Element and Gallium Diffusion in Yttrium Aluminum Garnet", Phys. Chem. Materials **26**, 156-163 (1998).
- <sup>viii</sup> W. D. Kingery, H. K. Bowen and D. R. Uhlman, Introduction to Ceramics, John Wiley and Sons, N.Y. pgs. 448-455 (1976).

## APPENDIX A

Cross sections, diffusion profiles and grain sizes



time →



## APPENDIX B

**Table 1.** Measured values of  $D_{eff}t$  for each diffusion experiment including the hold temperature and time, and calculated values using Eq. 3 and including diffusion during the ramp from 1050 C to the hold temperature and during the hold at sintering temperature. Calculations use the optimized values of parameters given in the text. Also in the table are grain sizes measured from fractured surfaces. Results are for all the samples measured in this study.

Sample number	Hold temp. (C)	Time (s)	Grain size ( $\mu\text{m}$ )	Exp. $D_{eff}t$ ( $\mu\text{m}^2$ )	Calc. ( $\mu\text{m}^2$ )
1	1600	240		7.8	4.5
2	1600	28800		39.1	27.1
3	1600	28800		36.4	27.1
4	1650	240		14.3	9.6
5	1650	240		14.7	9.6
6	1650	14400		76.4	36.7
7	1650	14400		50.1	36.7
8	1650	28800		64.3	49.6
9	1650	28800		81.2	49.6
10	1700	240		24.3	20.6
11	1700	240		24.0	20.6
12	1700	240		29.2	20.6
13	1700	14400		76.9	67.0
14	1700	14400	3	66.8	67.0
15	1700	28800		93.0	89.2
16	1700	28800	6	96.4	89.2
17	1750	240		46.4	44.5
18	1750	240		53.6	44.5
19	1750	14400		116.2	121.6
20	1750	14400		104.7	121.6
21	1750	28800		135.1	158.7
22	1750	28800		130.0	158.7
23	1780	240		78.9	71.7
24	1780	240	6	56.7	71.7
25	1780	14400	8	212.2	176.2
26	1780	28800		191.7	226.8
27	1780	28800	13	254.6	226.8